Supplemental Materials

High Electron Mobility and Large Magnetoresistance in the Half-Heulser Semimetal LuPtBi

Zhipeng Hou[1,2], Wenhong Wang[1,*], Guizhou Xu[1], Xiaoming Zhang[1], Zhiyang Wei[1], Shipeng Shen[1], Enke Liu[1], Yuan Yao[1], Yisheng Chai[1], Young Sun[1], Xuekui Xi[1], Wenquan Wang[2], Zhongyuan Liu[3], Guangheng Wu[1] and Xi-xiang Zhang[4]

[1]State Key Laboratory for Magnetism, Beijing National Laboratory for Condensed Matter Physics, Institute of Physics, Chinese Academy of Sciences, Beijing 100190, China

[2]College of Physics, Jilin University, Changchun 130023, China

[3]State Key Laboratory of Metastable Material Sciences and Technology, Yanshan University, Qinhuangdao 066004, China

[4]Physical Science and Engineering, King Abdullah University of Science and Technology (KAUST), Thuwal 23955-6900, Saudi Arabia.

[*] Corresponding author. wenhong.wang@iphy.ac.cn

S1

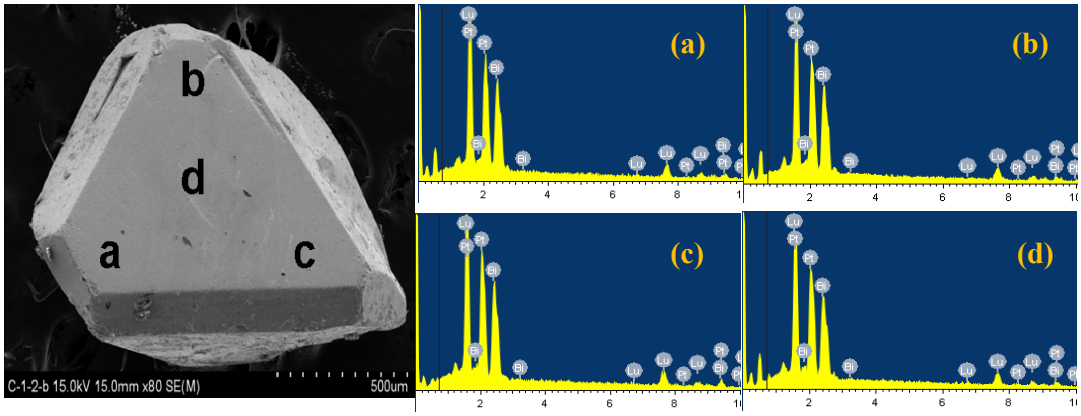

S5

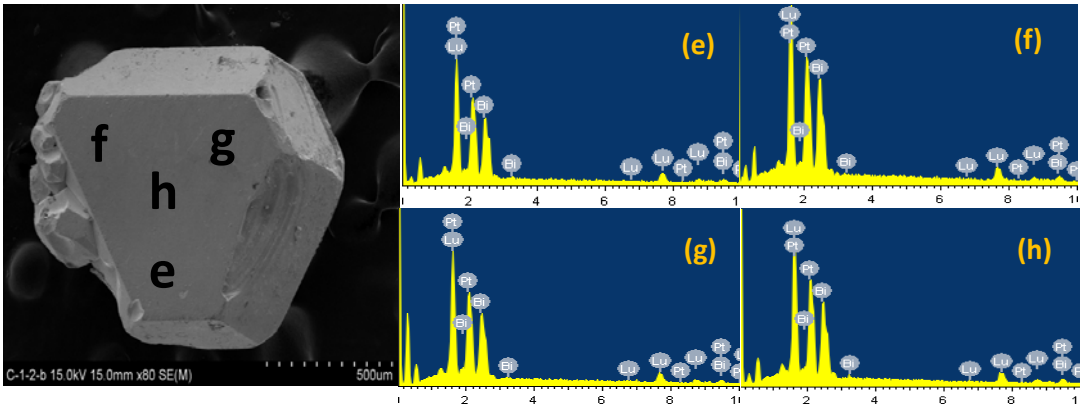

FIG. S1. EDX spectras of samples S1 (a, b, c, d) and S5 (e, f, g, h). EDX analyses were performed at numbered points on the crystal surface and the corresponding results are listed in Table S1. The average atom percentages of Lu: Pt: Bi were 31.96%: 32.94% : 35.10% and 31.94%: 33.43%: 34.63% for S1 and S5, respectively. Notably, EDX results are only semi-quantitative and a measurement error of 1- 2% should be considered.

S1			
Position	**Lu(at.%)**	**Pt (at.%)**	**Bi (at.%)**
a	**32.16**	**32.59**	**35.25**
b	**31.59**	**32.85**	**35.56**
c	**31.36**	**33.92**	**34.73**
d	**32.75**	**32.38**	**34.87**
Average	**31.96**	**32.94**	**35.10**
S5			
Position	**Lu (at.%)**	**Pt (at.%)**	**Bi (at.%)**
a	**31.86**	**33.69**	**34.45**
b	**31.83**	**33.59**	**34.58**
c	**31.88**	**33.38**	**34.74**
d	**31.77**	**33.45**	**34.78**
Average	**31.84**	**33.52**	**34.69**

Table S1. Chemical compositions of S1 and S5 samples determined by EDX at different positions of crystal surfaces.

Sample	t mm	ρ_{xx} μΩcm	RRR R_{300K}/R_{2K}	MR 2K, 10T	μ_e $cm^2V^{-1}s^{-1}$	μ_h $cm^2V^{-1}s^{-1}$	n_e $10^{19}cm^{-3}$	n_h $10^{19}cm^{-3}$
S1	0.21	3.70	4.3	3200%	79000	7320	2.0	3.7
S3	0.23	8.36	4.1	3000%	74000	5400	1.7	3.0
S5	0.19	22.7	3.4	1900%	31000	5000	1.2	2.5
S6	0.23	14.3	2.6	1000%	12000	4300	1.0	2.3
S9	0.21	24.5	2.3	353%	8200	2500	0.4	2.0
S12	0.25	76.8	1.4	136%	-	2400	-	3.0

Table S2. t is the thickness of the sample. ρ_{xx} is the resistivity at 2 K. *RRR* represents the ratio of ρ_{xx}(300 K)/ ρ_{xx}(2 K). The mobilities (μ_e and μ_h) and carrier concentrations (n_e and n_h) of S1, S3, S5, S6, S9 and S12 were established by two-carrier model but one-band model for S12 sample.

S2					
t (mm)	ρ_{xx} (μΩ cm)	RRR (R_{300K}/R_{2K})	MR (2 K, 10 T)	μ_e ($cm^2V^{-1}s^{-1}$)	μ_h ($cm^2V^{-1}s^{-1}$)
0.60	7.82	3.8	2800%	65000	5500
0.35	8.36	3.77	2650%	63500	5400
0.15	8.45	3.75	2600%	63000	5400
S6					
t (mm)	ρ_{xx} (μΩ cm)	RRR (R_{300K}/R_{2K})	MR (2 K, 10 T)	μ_e ($cm^2V^{-1}s^{-1}$)	μ_h ($cm^2V^{-1}s^{-1}$)
0.62	21.4	2.6	670%	11000	3800
0.43	22.5	2.56	640%	10800	3500
0.21	21.7	2.5	645%	10870	3450

Table S3. Thickness dependence of the transport parameters in samples S2 and S6.

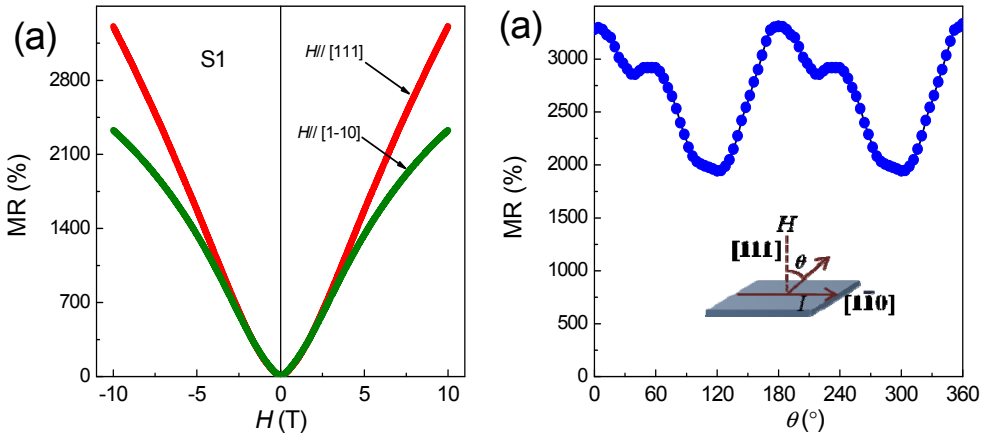

FIG. S2. (a) The MR ratio for Sample S1 at different orientations. The $\Delta\rho_{xx}(H)/\rho_{xx}(0)$ under a perpendicular magnetic field (*H* perpendicular to *I* and ab-plane) is shown by the red line, and $\Delta\rho_{xx}(H)/\rho_{xx}(0)$ at 2 K under a longitudinal magnetic field (*H* perpendicular to *I* and parallel to the ab-plane) is shown by the black line. At 2 K and under a magnetic field of 10 T, a transverse MR ratio of 3200% was obtained, while the longitudinal MR decreased to 2230%, indicating that the angle between the magnetic field and the [111] direction can affect the MR ratio. (b) Observed azimuthal field-angle dependence of the MR ratio of LuPtBi at 2 K and 10 T. Here, magnetic field *H* is rotated from the [111] to the [1-10] direction, as shown by the inset.

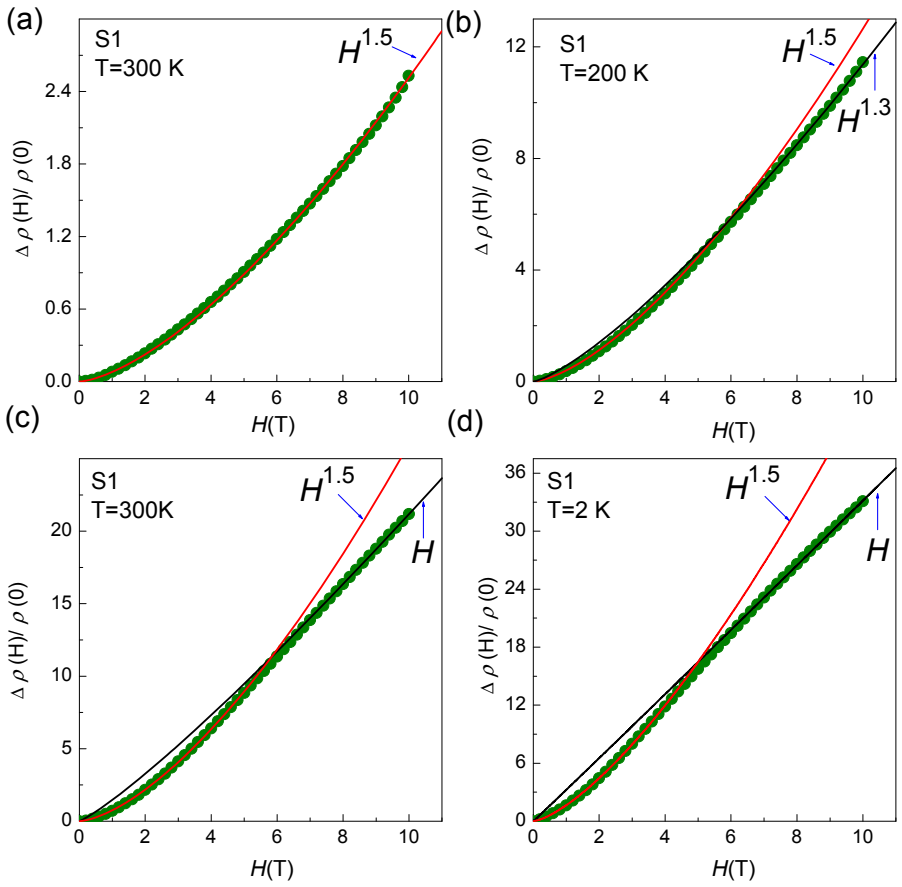

FIG. S3. The magnetic field dependence of the MR ratio $\Delta\rho_{xx}(H)/\rho_{xx}(0)$ for LuPtBi single crystals at a series of temperatures, T = (a) 300 K, (b) 100 K, (c) 50 K and (d) 2 K. Green circles are the experimental data and the solid lines (red and black lines) are fit data fit with MR = aH^b. At 300 K, MR can be fitted well with $aH^{1.5}$**Error! Reference source not found.**; however, MR at a high-field regime gradually deviates from $aH^{1.5}$**Error! Reference source not found.** with decreasing temperature and shows a linear MR behavior at low temperatures (between 50 K and 2 K) and high-field regimes.

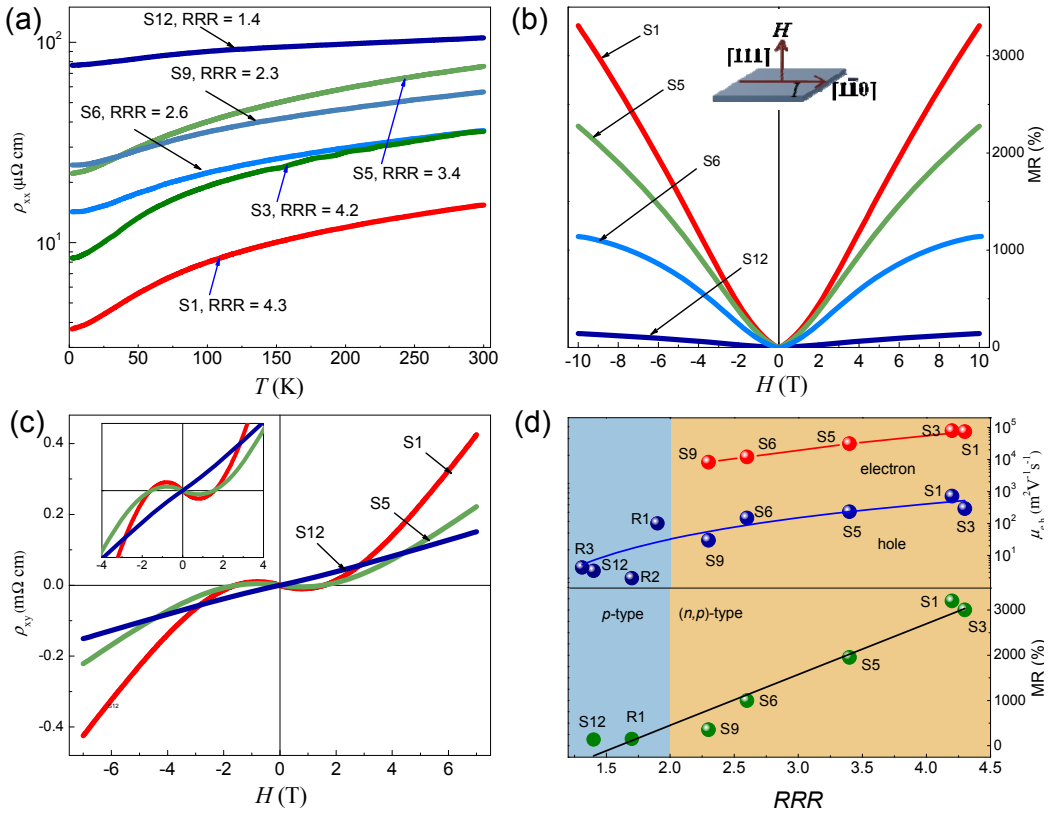

FIG. S4. (a) Temperature dependence of zero-field resistivity ρ_{xx} curves for six representative crystals with various RRRs. (b) MR curves for samples S1, S5, S6 and S12 measured at 2 K. (c) Hall resistivity ρ_{xy} curves for samples S1, S3, and S12 measured at 2 K. The upper inset shows an expanded view of the low H region, and the lower inset is a high-resolution STEM image for sample S3. (d) Upper plane: electron (red solid) and hole (blue solid) mobilities versus RRR. Lower plane: MR values (green solid) versus RRR. Orange represents the coexistence of electron and hole carriers, whereas the blue region indicates a hole-dominated transport region.

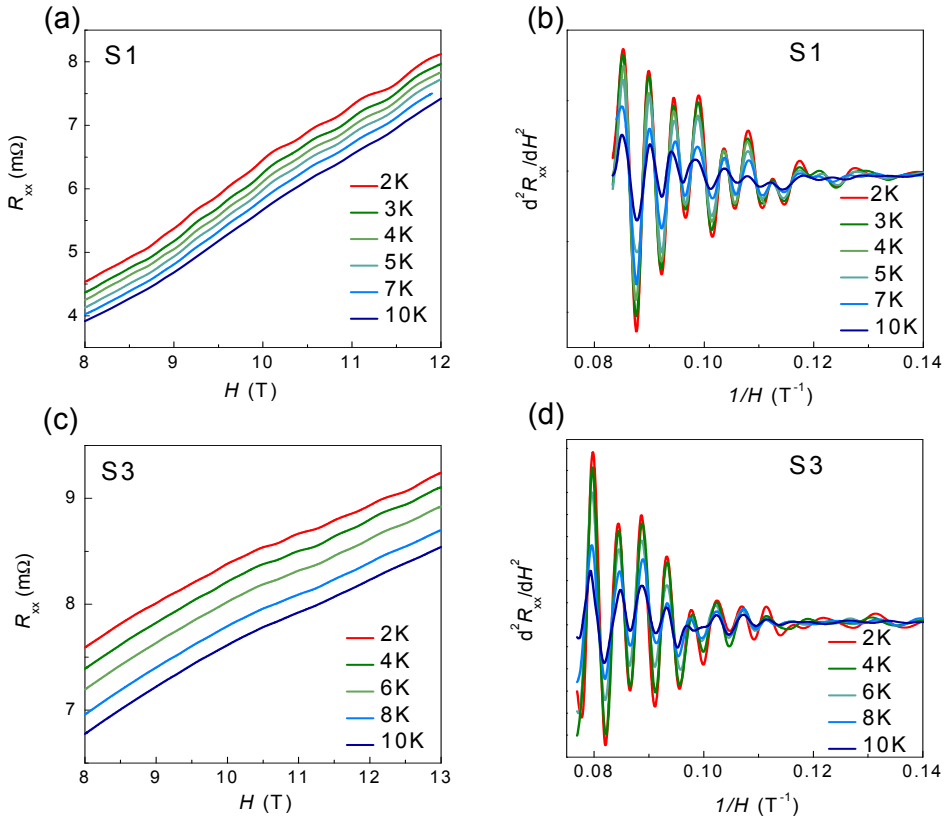

FIG. S5. The temperature dependence of SdH quantum oscillations at high magnetic fields for samples S1 and S3. The field is applied perpendicular to the [111] direction. At high fields, as shown in (a) and (b), the clear SdH oscillations are superimposed on a huge background of positive MR. The oscillations become apparent in the second derivative d^2R_{xx}/dH^2 as a function of the inverse magnetic field $1/H$ as shown in (c) and (d).

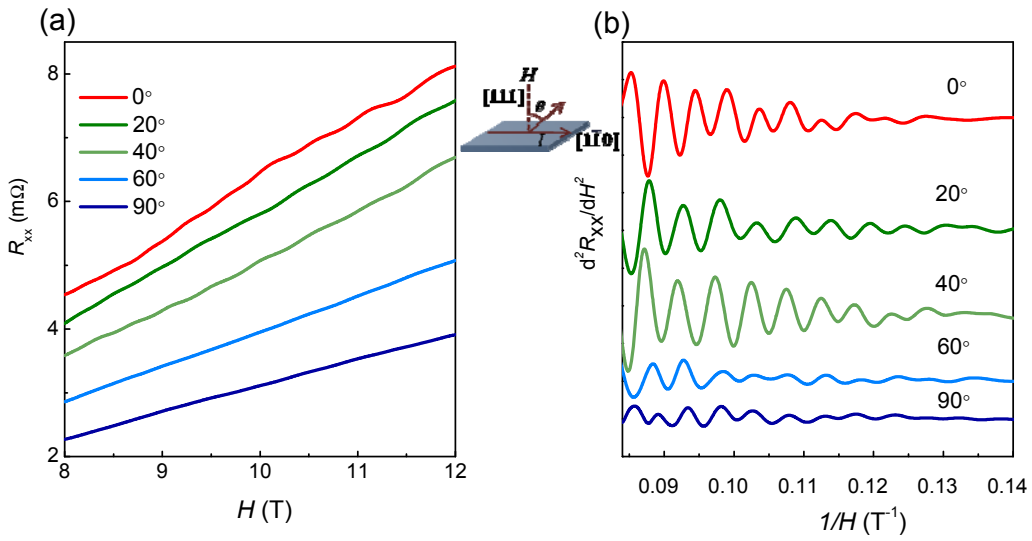

FIG. S6. (a) Angle dependence of resistance of sample S1 at high fields. The magnetic field H is rotated in the z-y plane as shown in the inset. When we rotate the angle θ from the [111] to the [1-10] direction, as shown in (b), distinct SdH oscillations are observed in the second derivative d^2R_{xx}/dH^2 as a function of the inverse magnetic field $1/H$.

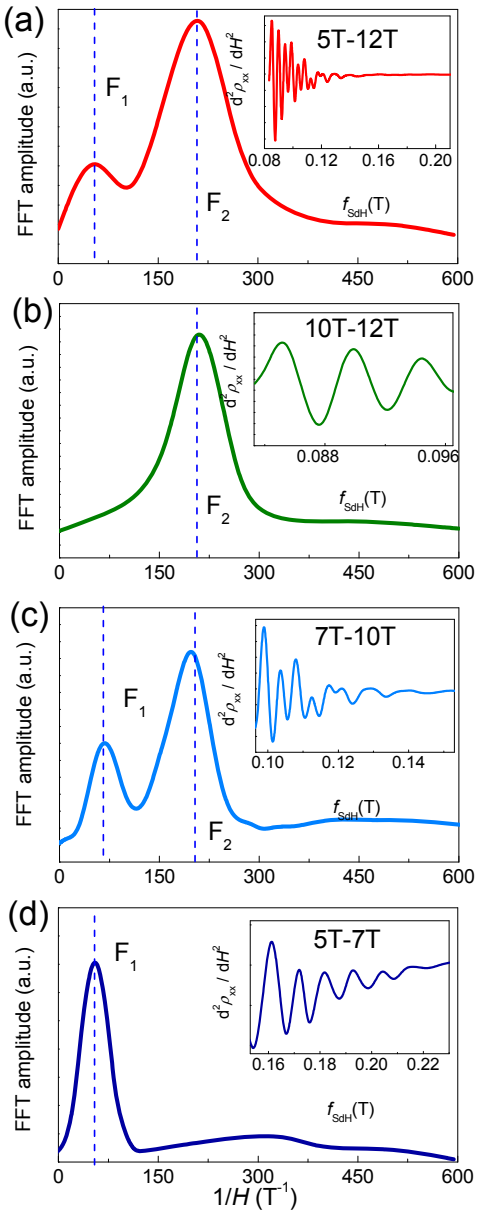

FIG. S7. (a) FFT in the magnetic field range of 5T-12T, two peaks at F_1=80 T and F_2=200 T are found. (b) FFT in the magnetic field range of 10 T – 12 T, only one peak at F_2=200 T is found. Since the holes carriers dominate the transport properties at high fields, the F2 peak corresponds to the SdH oscillations of hole. (c) FFT in the magnetic field range of 7 T - 10 T, F_1 at 80 T together with F2 peak appear. (c) FFT in the magnetic field range of 5 T – 7 T, only F_1 peak can be found. Since the electron exhibits higher mobility, it should show SdH oscillations at lower magnetic field. Therefore, the F1 peak corresponds to SdH oscillations of electron.